Electronic Excited States of D-(−)-Luciferin and Related Chromophores

Jin Jung, Chen-An Chin, and Pill-Soon Song*

Contribution from the Department of Chemistry, Texas Tech University, Lubbock, Texas 79409. *Received June 7, 1975*

Abstract: The fluorescent state of D-(−)-luciferin (LH_2) and related compounds is characterized by a strong charge transfer from the hydroxybenzothiazole to the thiazoline ring, resulting in large lowering of the pK_a of the hydroxyl group, increase in the S_1 dipole moment, and strong solvent and temperature dependence of the Stokes' shift. The polarization of the S_1 transition for all luciferyl compounds studied is along the long molecular axis, according to the MO calculations. The fluorescence polarization of LH^- is significantly higher than that of LH_2 under identical conditions in the absence of rotational depolarization. This is interpreted by a better linear oscillator approximation in LH^- than in LH_2 due to the strong charge transfer nature of the LH^- fluorescence. The phosphorescence of LH_2 is mixed, in-plane and out-of-plane polarized, with a lifetime of 0.028 s. The T_1 state assignment is $^3(\pi,\pi^*)$. Configuration analysis of the T_1 states of luciferyl compounds suggests that the lowest triplet state is either delocalized or localized in one of the ring systems without significant charge transfer, contrary to the fluorescent states.

The bioluminescence reaction in firefly extracts is now well understood, both in terms of the enzymatic scheme[1] and reaction mechanisms.[2-5] Although LH_2 itself does not appear to be the *emitting* species of the firefly bioluminescence,[2] the chromophore responsible for the bioluminescence emission (i.e., decarboxyluciferin anion[2]) shows spectroscopic characteristics similar to those of LH_2 and dehydroluciferin (L), as far as the 6′-hydroxybenzothiazole chromophore is concerned.[6] In fact, LH_2 anion (LH^- phenolate form) shows emitting characteristics (e.g., fluorescence quantum yield and emission maximum) similar to the bioluminescence chromophore.[6] The present work examines the electronic structure of the excited states of LH_2 and other firefly bioluminescence chromophores in order to elucidate their spectroscopic relationships. Structures concerned are shown below.

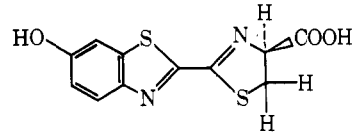
D (−)-Luciferin (LH_2)

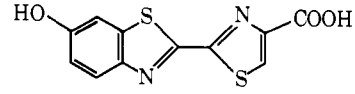
Dehydroluciferin (L)

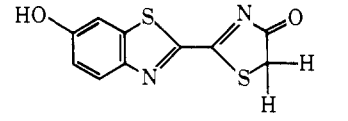
Oxyluciferin ($oxyL^-$)

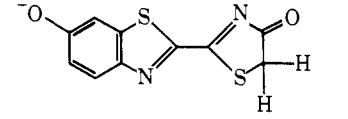
Oxyluciferin monoanion ($oxyL^-$)

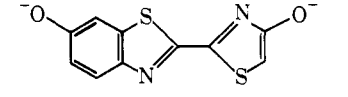
Oxyluciferin dianion ($oxyL^{2-}$)

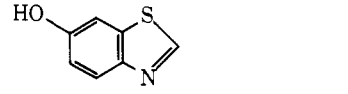
Hydroxybenzothiazole (I)

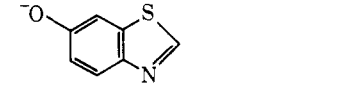
Hydroxybenzothiazole anion (I^-)

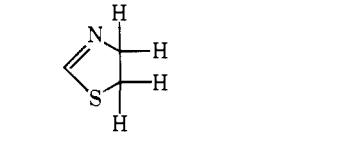
Thiazoline (II)

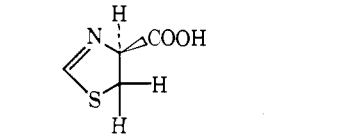
Thiazolinecarboxylic acid (II COOH)

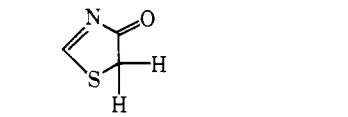
Oxythiazoline (II_o)

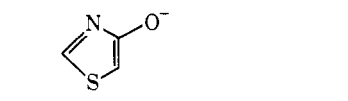
Oxythiazoline enolate (II_o^-)

Experimental Section

Materials. Two different batches of D-(−)-luciferin (LH_2) were purchased from Sigma Chemical Co. The first batch of the material was purified by TLC (solvent; chloroform–*n*-butyl alcohol–water, 1:9:3.3 v/v, or *tert*-butyl alcohol–methyl ethyl ketone–water–ammonium hydroxide, 4:3:2:1, v/v, on Eastman cellulose-coated chromatogram sheets) prior to its use, as it contained luminescent impurities. The second batch obtained was found to be free of luminescent impurities, and its purity was ascertained by recording the fluorescence emission and excitation spectra at varying combinations of the excitation and detection wavelengths. Absolute ethanol (U.S. Industry) was fractionally distilled to remove most of the luminescent impurities. Water was deionized and redistilled, while all other solvents were spectrograde. Potassium hydroxide was obtained from J. T. Baker Chemical Co. and ethanolic KOH was free of luminescent impurities at the desired sensitivity setting of the luminescence detector.

Preparation of phenolate ion (LH^-) of D-(−)-luciferin was carried out by dissolving LH_2 in ethanolic KOH (saturated) which had been purged with nitrogen for 20 min to avoid the oxidation of LH_2 in alkaline solution.[7]

Phenolate ion formation was followed by the absorption increase at 287 and 396 nm (new bands), while the absorption bands of LH_2 at 269 and 328 nm decreased with increasing KOH concentrations (Figure 1). The original LH_2 spectrum was readily recovered by neutralizing the solution with HCl. At the KOH saturation point, all LH_2 was converted to LH^-.

Methods. Unless otherwise indicated, all measurements were carried out at 77 K using specially designed Dewars. Absorption spectra were recorded on a Cary 118C spectrophotometer. Fluorescence, phosphorescence, polarization, and phosphorescence lifetime were measured as described previously.[8] Corrected luminescence spectra were measured on a Perkin-Elmer spectrofluorometer Model MPF-3. A high resolution spectrofluorometer with single-photon counting

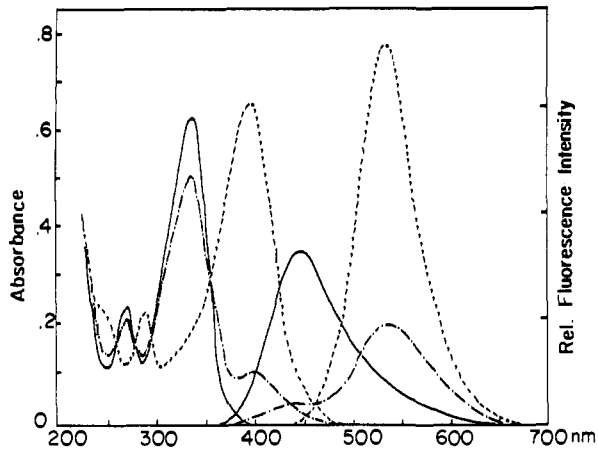

Figure 1. Absorption (left) and fluorescence (right) spectra of D-(−)-luciferin in ethanol at room temperature. (—) no KOH added; (-·-·-); 0.001 M KOH; (- - -) 0.015 M KOH. Band pass for excitation and emission was 2 and 1 nm, respectively.

Table I. Semiempirical Integrals (in eV) for PPP Calculations

Atom	Ionization potential ($-W_{2p}$)	$\langle rr\|rr\rangle$	β_{cx}
C	11.16	11.13	−2.39
N	14.12	12.34	−2.39
S	22.88	12.14	−1.40
O	32.90[a]	21.53	−2.12

[a] For phenolate oxygen, ionization potential was taken as 26.14, which was calibrated with reference to the uv absorption maxima of hydroxy pyridine anions.

mode[8] was used for some of the low-temperature measurements (e.g., polarization). The CD spectrum of D-(−)-LH_2 was recorded on a JASCO-J20 CD-ORD spectrometer which was modified to enhance the signal-to-noise ratio by replacing the Pockel cell and circuitry with a Morvue photoelastic modulator (PEM-3) and lock-in amplifier/phase detector (PAR Model 121).

Theoretical Section

SCF MO CI Pariser–Parr–Pople (PPP) Computations. Transition energies, oscillator strengths, polarization directions, and other electronic indices were calculated by the standard PPP procedure,[9] as used previously.[10]

Table I lists parameters which are commonly used in similar calculations of heterocyclic systems. The two-center electron repulsion integrals, $\langle rr|ss\rangle$, were calculated according to Mataga and Nishimoto.[11] Thirty singly excited configurations were included in the configuration interaction matrix. The input geometry of the luciferin π-electron framework was based on crystallographic data.[12]

Configuration Analysis (CA). The CA method expresses the SCF CI wave functions (Ψ) of the molecule in question in terms of the corresponding wave functions (Ψ^0) of "reference" orbitals,[13] $\Psi = \Psi^0 M$, where M is an appropriate transformation matrix[13] (see Appendix).

Thus, wave functions of composite and bichromophoric systems such as LH_2 [hydroxybenzothiazole (I) + thiazoline (II)] can be quantitatively analyzed in terms of the wave functions of reference molecular fragments. The CA method is most suitable for the present objective, i.e., to analyze and correlate the spectroscopic characteristics of various forms of firefly luciferins.

Results and Discussion

Excited Singlet States: π–π^* Transitions. Figure 2 shows the absorption spectrum of LH_2 in ethanol at 77 K, along with the PPP results of the $\pi \rightarrow \pi^*$ transition energies and oscillator strengths. The uv spectrum of LH_2 (Figure 2) is accounted for in terms of the calculated low energy $\pi \rightarrow \pi^*$ transitions which are in good agreement with the observed band maxima, except for the fourth transition (observed at 234 nm; predicted at 248 nm).

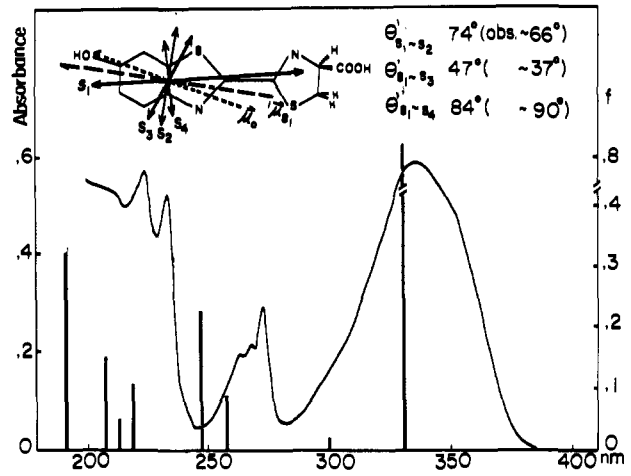

Figure 2. Absorption spectrum of LH_2 in ethanol at 77 K. The calculated spectrum (energy and oscillator strength, f) is indicated by vertical lines. The calculated polarization directions of S_1–S_4 and permanent dipole moments (μ_0 and $^1\mu_{S_1}$) are also shown, along with comparison of polarization angle (between fluorescent oscillator and higher singlet oscillators), calculated from the Levshin–Perrin equation and by correcting for the depolarization of the fluorescence (Figure 4).

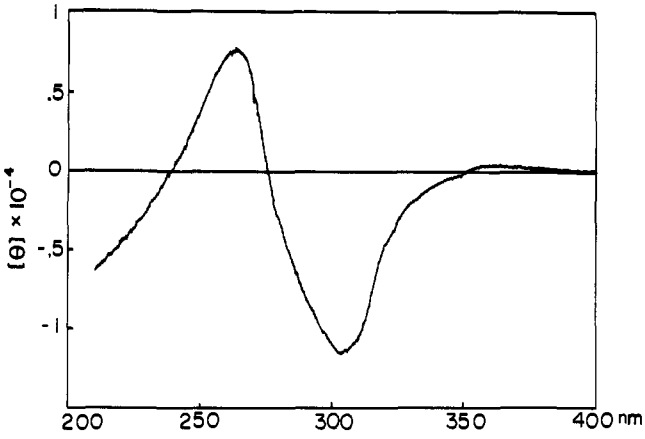

Figure 3. Circular dichroic spectrum of LH_2 (2×10^{-5} M) in ethanol at room temperature.

The presence of a transition predicted at 302 nm (short wavelength tail region of the main absorption band) is confirmed by the CD spectrum, which clearly shows a distinct (−)-ellipticity band at the same wavelength (Figure 3). Apparently, the molar ellipticity of the main absorption band at 334 nm is too small to resolve its CD band. There is a very weak (+)-ellipticity in the long wavelength edge. This may be an indication of the positive CD band for the main absorption, although its validity cannot be ascertained until a time-average computing measurement is performed.

The polarized fluorescence excitation spectrum (Figure 4) further confirms the weak band ($S_0 \rightarrow S_2$ at ~300 nm) as the degree of polarization decreases significantly toward the 300-nm region. The first two transitions are polarized in substantially different directions (cf. Figures 3 and 4). This is further confirmed by the MO calculations (Figure 2). Relative polarization assignments are determined from the Levshin–Perrin equation[14,15]

$$P = (3\cos^2\theta' - 1)/(\cos^2\theta' + 3)$$

Table II. The $\pi \rightarrow \pi^*$ Transitions Calculated by the SCF MO Method (PPP)

Compd	Transition	Energy, nm (obsd)	Oscillator strength (obsd)	Polarization axis[c]
LH_2	$S_0 \rightarrow S_1$	331 (334)[a]	0.822 (0.433)[a]	Long, Fig 2
	S_2	302 (~300)[b]	0.020	Short, Fig 2
	S_3	258 (273)[a]	0.087 (0.096)[a]	~Short, Fig 2
	S_4	248 (234)[a]	0.237 (~0.6)[a]	Short, Fig 2
	S_5	220 (225)[a]	0.109	Long
LH^-	$S_0 \rightarrow S_1$	407 (384)[a]	0.823	Long
	S_2	337	0.043	Short
	S_3	275 (285)[a]	0.114	Interm
	S_4	252	0.323	Interm
	S_5	240	0.242	Long
L	$S_0 \rightarrow S_1$	389 (348)[d]	0.853	Long
	S_2	322	0.031	Short
	S_3	285 (273)	0.017	Long
	S_4	257	0.095	Short
	S_5	253	0.001	Interm
Dehydroluciferol	$S_0 \rightarrow S_1$	401	0.855	Long
	S_2	319	0.041	Short
	S_3	298	0.025	Short
	S_4	258	0.056	Short
	S_5	238	0.267	Interm
Oxyluciferin monoanion	$S_0 \rightarrow S_1$	456 (432)[e]	1.054	Long
	S_2	334	0.027	Short
	S_3	297	0.136	Long
	S_4	276	0.497	Interm
	S_5	254	0.171	Long
Oxyluciferin dianion	$S_0 \rightarrow S_1$	532	0.253	Long
	S_2	371	0.582	Long
	S_3	347	0.119	Long
	S_4	273	0.065	Long
Hydroxybenzothiazole	$S_0 \rightarrow S_1$	358 (298)[7]	0.097	Interm
	S_2	305	0.541	Long
	S_3	236	0.103	Short
LH_2	$T_1 \rightarrow S_0$	671 (564)[f]	0	
	T_2	460	0.073	Long
	T_3	382	0.001	Interm
	T_4	368	0.088	Long
	T_5	323	0.011	Short

[a] Absorption maxima in ethanol at 77 K. [b] From CD spectrum taken at room temperature (Figure 3). [c] Approximate range of polarization direction. "Intermediate" implies a polarization axis between long- and short-molecular axis (cf. with the insert in Figure 2). [d] Observed.[6] [e] Observed.[4b] [f] Observed λ_{max}^P, Figure 1.

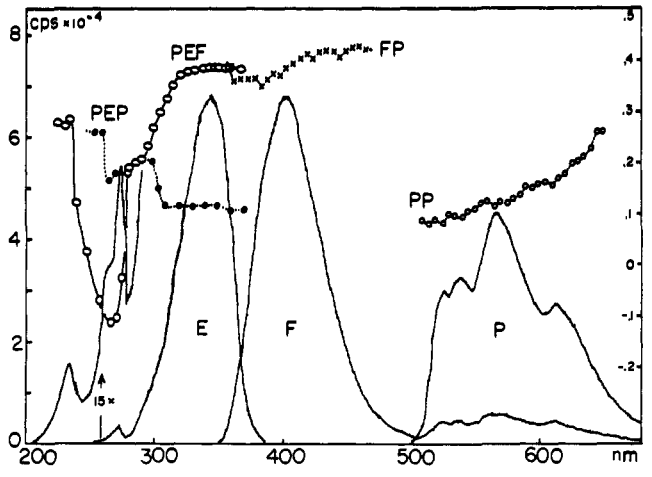

Figure 4. Emission (F, fluorescence; P, phosphorescence) and excitation (E) spectra of LH_2 in ethanol at 77 K; recorded intensity in counts per second on a high-resolution, single-photon counting spectrometer without spectral corrections. Polarization of fluorescence emission (FP, λ_{ex} ~350 nm) and excitation (PEF, λ_F ~550 nm) refers to the right ordinate. All spectra were recorded at bandpass less than 0.2 nm. The higher phosphorescence spectrum was recorded with a phosphoroscope.

where θ' is the angle between the absorbing and emitting oscillators. The calculated polarization diagram is shown in Figure 2. The long absorption band is predicted to be polarized along the long molecular axis. This prediction has an important implication concerning the electronic structure of the lowest π,π^* state of LH_2 (e.g., the dipole moment of the excited state and its orientation, configuration analysis; vide infra).

Table II presents the calculated transition data for LH_2, LH^-, L, oxyluciferin monoanion, and hydroxybenzothiazol In all cases, the lowest energy transition is the most intense transition with polarization along the long molecular axis, except for hydroxybenzothiazole. From Tables II and III, the S_1 state in luciferyl chromophores is correlated with the S_2 state of hydroxybenzothiazole, since the S_2 of the latter is most intense and is long-axis polarized. This qualitative reasoning is further supported quantitatively by the configuration analysis data shown in Table III. Thus, CA of the S_1 state of LH_2, L, and oxyluciferin monoanion indicates predominant contributions of the S_2 configuration of hydroxybenzothiazole moiety to the former. In addition, a significant charge transfer from hydroxybenzothiazole to thiazoline moiety is characteristic of the S_1 state wave functions of these luciferyl chromophores. The oxyluciferin dianion, however, shows a substantial localization of the S_1 state in the thiazoline anion, as well as 26% charge transfer contribution from the thiazoline to the benzothiazole anion ring (Table III).

Fluorescence of Luciferins. Fluorescence properties of luciferyl compounds have been studied extensively by Morton et al.[6] Fluorescence of these compounds is mainly from the corresponding phenolate anion forms in aqueous solutions,

Table III. Configuration Analysis for Luciferyl Compounds in the Singlet (S_1) and Triplet (T_1) Excited States (wt %)[f]

Compd (see structures)	Reference state	State function Ψ_1	
		S_1	T_1
LH_2	Ψ_1^0 (6 → 10)[a]	21.7	40.0
	Ψ_2^0 (6 → 11)	40.9	2.6
	Ψ_3^0 (6 → 12)	3.5	0.1
	Ψ_{20}^0 (8 → 9)	0.2	31.7
	Ψ_{21}^0 (7 → 9)	3.1	0.0
	Ψ_{CT}^0 (7 → 10)[b]	2.6	3.8
	Ψ_{CT}^0 (8 → 10)	0.1	5.2
	Ψ_{CT}^0 (6 → 9)	20.3	9.8
	Ψ_{CT}^0 (5 → 9)	1.9	0.0
	Ψ_{CT}^0 (4 → 9)	1.3	3.2
	Total weight	91.3	93.0
L	Ψ_1^0 (6 → 15)[c]	15.8	80.2
	Ψ_2^0 (6 → 16)	33.7	1.1
	Ψ_3^0 (6 → 17)	0.5	2.7
	Ψ_5^0 (5 → 16)	0.5	1.8
	Ψ_8^0 (5 → 18)	0.0	2.6
	Ψ_{13}^0 (11 → 12)	6.9	0.6
	Ψ_{CT}^0 (6 → 12)	18.8	4.1
	Ψ_{CT}^0 (6 → 13)	9.9	3.0
	Total weight	87.9	87.1
$OxyL^-$	Ψ_1^0 (6 → 12)[d]	9.2	83.2
	Ψ_2^0 (6 → 13)	40.8	0.5
	Ψ_3^0 (6 → 14)	0.3	2.5
	Ψ_{15}^0 (9 → 11)	2.7	0.0
	Ψ_{CT}^0 (6 → 10)	33.9	10.1
	Ψ_{CT}^0 (4 → 10)	1.8	0.1
	Total weight	85.4	85.6
$OxyL^{2-}$	Ψ_1^0 (6 → 13)[e]	0.2	3.7
	Ψ_{21}^0 (10 → 11)	64.8	70.3
	Ψ_{22}^0 (10 → 12)	0.4	10.6
	Ψ_{CT}^0 (10 → 13)	26.0	5.1
	Total weight	85.9	86.2

[a] Molecular orbitals 6 and 8 are the highest occupied MO's of hydroxybenzothiazole (I) and thiazoline (II) moieties, respectively, whereas MO's 10 and 9 are the lowest empty MO's for I and II, respectively, in the case of CA for LH_2. [b] Charge transfer (CT) state arises from the electron transfer promotion from an MO of one moiety (I or II) to an MO of the other moiety (II or I, respectively). The similar intermoiety electron transfers give rise to CT states in other compounds. [c] HOMO's for I and II-COOH are labeled b and 11, respectively, whereas LEMO's for I and II-COOH are 15 and 12, respectively, in the case of CA for L. [d] HOMO's for I^- and II_0 are labeled 6 and 9, respectively, whereas LEMO's are labeled 12 and 10, respectively, in the case of CA for $oxyL^-$. [e] HOMO's for I^- and II_0^- are labeled 6 and 10, respectively, whereas LEMO's are labeled 13 and 11, respectively, in the case of CA for $OxyL^{2-}$. [f] Only those reference functions contributing > ~2% are listed.

while the neutral forms are relatively nonfluorescent.[6] In protic solvents, the former is produced in the fluorescent state because of the lowering of the hydroxyl pK_a upon excitation. For example, the pK_a* of LH_2 is estimated as <0, whereas the pK_a is 8.4 ± 0.2[16] to 8.7.[6] Using approximate 0-0 fluorescence frequencies, $\bar{\nu} \simeq \frac{1}{2}(\bar{\nu}_{abs\ max} + \bar{\nu}_{fluor\ max})$, for neutral (in ethanol) and anionic species (pH 11.5, Figure 5) and by applying the well-known Förster cycle,[17] we obtain a pK_a* value of −0.19. A value of −0.87 is obtained by using the 0-0 frequencies of the neutral and anionic species in ethanol and ethanolic KOH, respectively (Figure 1). These estimates confirm that the hydroxyl proton becomes considerably more acidic in the fluorescent state than in the ground state of luciferyl compounds.[6,16,18]

The lowering of the hydroxyl pK_a upon excitation is predictable on the basis of the decrease in electron density. Thus, the electron density on the hydroxyl oxygen decreases from 1.910 in the ground state to 1.835 in the S_1 state of LH_2, thus lowering its pK_a.

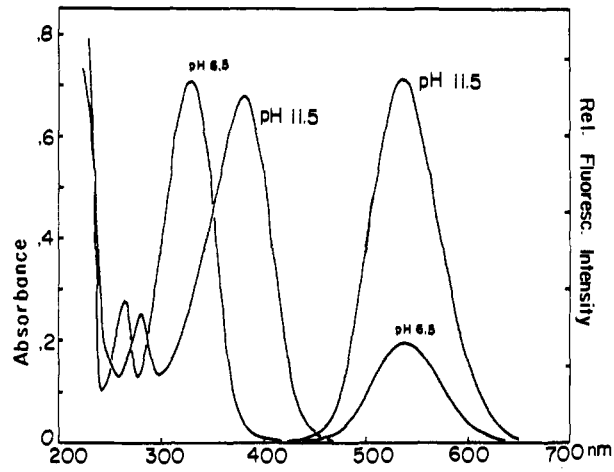

Figure 5. Absorption (left) and fluorescence (right) spectra of LH_2 in aqueous solutions (pH indicated) at room temperature. The fluorescence spectra were corrected.

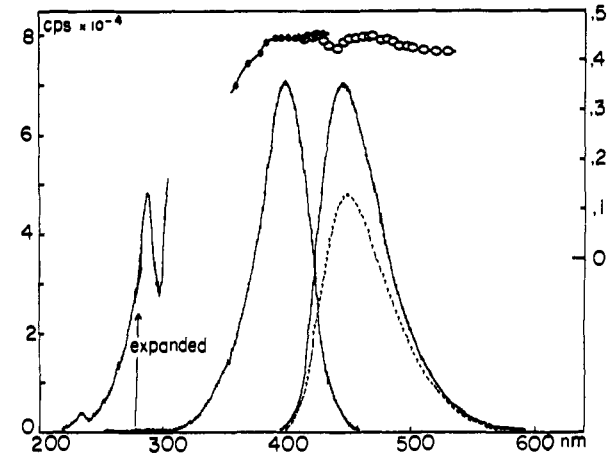

Figure 6. The fluorescence emission and excitation spectra of LH^- in ethanolic KOH at 77 K recorded on a high-resolution, single-photon counting spectrometer at a bandpass 0.4 nm. Manually corrected fluorescence spectrum (- - -) is also shown. The polarization is with respect to λ_{ex} ~395 nm (-●-) and λ_F ~445 nm (-○-).

Oxyluciferin anion is apparently the light emitting species in bioluminescence (particularly red light).[2] The acidity of the hydroxyl proton in the excited oxyluciferin (electron density ~1.552 in S_0 and 1.287 in S_1 state) is predicted to be even higher than that of LH_2. Thus, it appears that lowering of the hydroxyl pK_a characterizes the fluorescent state of not only LH_2 but its related derivatives (dehydroluciferin, dehydroluciferol, and oxyluciferin; MO results available upon request).

Another characteristic feature of luciferyl fluorescence is the strong dependence of the emission maximum on temperature and solvent polarity. The fluorescence maximum of LH_2 is at 444 nm in ethanol at room temperature (Figure 1), and shifts to 404 nm at 77 K (Figure 4). LH^- behaves in the same way, the fluorescence maximum being shifted from 532 nm at room temperature to 450 nm at 77 K (Figures 1 and 6). It should be noted that the blue shift observed is contrary to the dispersion shift due to the increased refractive index of the medium at 77 K.

The large solvent Stokes' shift in LH_2 and LH^-, as well as other luciferyl compounds studied by Morton et al.,[6] can be accounted for in terms of solute-solvent dipole-dipole relax-

Table IV. Calculated π Dipole Moments (in Debyes)

Compd	μ_0	μ_{S_1}	μ_{T_1}
LH_2	1.54	12.45	3.12
LH^-	6.47	21.96	12.05
L	3.90	10.30	6.13
Dehydroluciferol	0.40	3.15	2.43
Oxyluciferin monoanion	10.70	26.85	17.04

ations. Such dipole-dipole relaxations may contribute to the observed Stokes' shift, as predicted by the large increase in dipole moments of the luciferyl chromophores (Table IV).

In order to examine the nature of the large Stokes' shift as a function of temperature and solvent polarity described above, solvent dependence of the emission maximum of LH_2 was studied. Figure 7 shows an example of the solvent shift. It can be seen that the large blue shift (2353 cm^{-1}) of the emission maximum occurs in going from ethanol to *p*-dioxane, although the absorption maximum remain about the same (328 nm in ethanol and 326 nm in *p*-dioxane). Similar dependence has been noted with other solvent systems.

An approximate estimate of the S_1 state dipole moment of LH_2 can be made from the solvent dependence of the absorption and fluorescence maxima. By combining the solvent shift theories of Bakhshiev[19] and Chamma and Viallet,[20] it is possible to calculate an approximate excited state dipole moment,[21] yielding 13.4 D for LH_2.[22] The excellent agreement between the "observed" and calculated dipole moment of the S_1 state (see Table IV) should not be taken quantitatively, since the observed estimate is subject to assumptions adopted[19-22] and σ-dipole contribution was not taken into account in the calculation presented in Table IV. Nonetheless, the dipolar nature of the fluorescent state of LH_2 and possibly other derivatives (e.g., LH^-) responsible for the Stokes' shift is qualitatively consistent with the data described above. The large suppression of the Stokes' shift of LH_2 and LH^- at low temperature can also be explained by the restricted dipole-dipole relaxation in the rigid matrix.

The greater dipole moment of S_1 relative to that of S_0 is apparently associated with a strong charge transfer (CT) from hydroxybenzothiazole to thiazoline ring, as suggested by the CA data (Table III). For example, the CT is negligible in S_0, but total CT is 24.3% for LH_2 and 36.6% for oxyluciferin monoanion (Table III). The electron density and bond order distributions in S_1 clearly reflect the CT character of the fluorescent state (MO data available upon request). As expected, the CT contribution in oxyluciferin dianion is negligible (Table III). The hydroxyl group plays an important role in determining the CT character of the fluorescent state of LH_2 and related species. Thus, large lowering of the pK_a, increase in dipole moment, long axis orientation of the transition moment, and μ_{S_1} of the fluorescent state are determined by the hydroxyl substituent to a significant extent.

Although the fluorescence spectrum of LH_2 at 77 K was not resolved (Figure 4), a high-resolution, single photon counting measurement of the polarized fluorescence shows some vibrational resolution which was reproducible (Figure 8). The approximate vibrational frequency resolved corresponds to 1250 ± 50 cm^{-1}. This may be assigned to the C-O stretching mode,[23] as predicted by the C-O bond shortening (and increase in bond order) in the fluorescent state.

It is also noteworthy that the fluorescence polarization of LH^- is consistently higher than that of LH_2 (Figure 6). This may well be a reflection of the strong CT contribution to the linear oscillator component of the absorption and emission anisotropy.

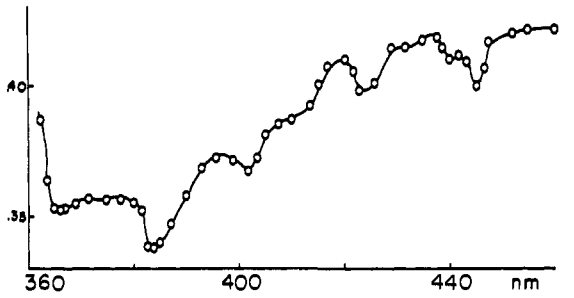

Figure 7. Polarized fluorescence spectrum of LH_2 in ethanol at 77 K (λ_{ex} ~350 nm) recorded on a high-resolution, single-photon counting spectrometer.

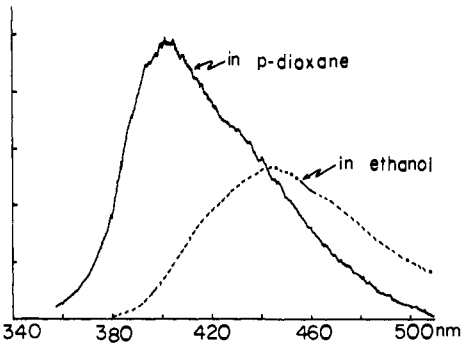

Figure 8. Corrected fluorescence spectra of LH_2 in two different solvents at room temperature. Bandpass ~2 nm.

Concluding this section, we note that all of the electronic features discussed above seem to be shared by luciferyl compounds, including the emitting species of bioluminescence (oxyluciferin anions). However, further spectroscopic data are needed for elucidating the singlet excited states (oscillator strength, polarization, and Stokes' shift, etc.) of bioluminescent intermediates which are not readily available for in vitro spectral measurements.

Triplet States. LH_2 shows phosphorescence (Figure 4). However, no phosphorescence was detectable for LH^- with the single photon counting spectrometer. The phosphorescence of LH_2 is short axis in-plane and out-of-plane (about 30-40°) polarized, since the polarized phosphorescence excitation at the 260-nm region (short axis polarized; cf. Figures 1 and 2) shows a relatively high degree of polarization. The singlet-triplet split is about 6000 cm^{-1}. The lifetime of the phosphorescence is 0.028 s. On the basis of these data and theoretical predictions of the energy of the lowest triplet state (Table II), the phosphorescent state of LH_2 is assigned as $^3(\pi,\pi^*)$ type. For triplet-triplet transitions calculated by the PPP method (Table II), there are no experimental data available for comparison.

LH^- is apparently not phosphorescent in the spectral region examined (500-900 nm). The calculated triplet state is at >1000 nm. Thus, failure to detect the phosphorescence can be ascribed to either the blue shift of an intermediate $^3(n,\pi^*)$ state or to a drastic lowering of the T_1 state. A similar situation applies to oxyluciferin and dehydroluciferin anions.

Unlike the S_1 states of luciferyl compounds, the T_1 state of LH_2 is more or less evenly delocalized over the two ring systems, without significant CT character (Table III). On the other hand, the T_1 states of dehydroluciferin and oxyluciferin monoanion are largely localized in the benzothiathole ring (Table IV). The T_1 state of oxyluciferin dianion is almost exclusively localized on the thiazoline moiety. In general, the calculated electronic structure of T_1 of luciferyl compounds is not as drastically different from that of the ground state as is S_1 (unpublished).

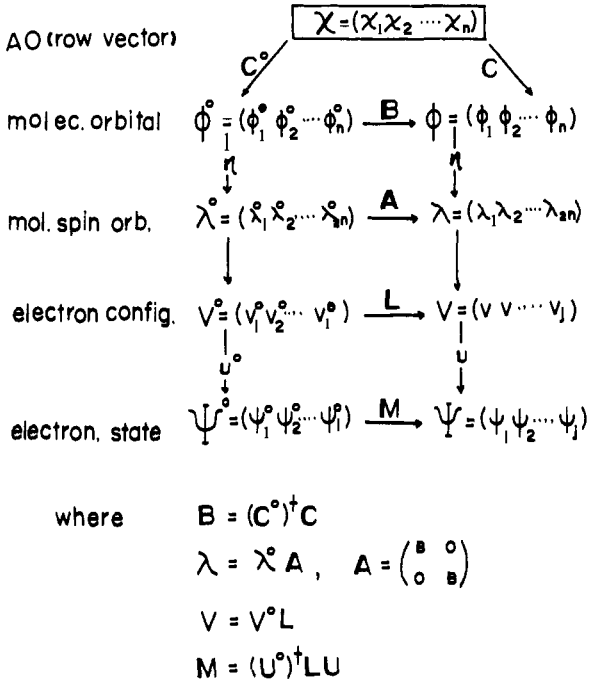

Figure 9. Schematic outline of the CA procedure.

Concluding Remarks

Spectroscopic properties such as relative energies and intensities, polarization, and fluorescence are similar for LH_2 and its derivatives, including bioluminescent intermediate species (oxyluciferin anions), as revealed from experimental and theoretical analyses described above. The fluorescent state of LH_2 and related compounds is characterized by a strong CT nature from the hydroxybenzothiazole to thiazoline ring, resulting in large lowering of the pK_a, dipolar electron distribution, and Stokes' shift which depends strongly on solvent polarity and temperature. If the LH_2 is enzymatically activated prior to the oxygenation, its transition state may have some CT character analogous to the S_1 state.

Of particular interest from the present study is the large dipole moment of the fluorescent state of LH_2 (and other derivatives). Thus, variations of bioluminescence maxima among different species and preparations can be accounted for in terms of luciferyl-apoprotein dipole-dipole relaxations which depend on mutual orientations of the dipoles involved and rigidity of the binding. Predicted orientation of the dipole moment of S_1 in oxyluciferin monoanion is along the long molecular axis, as in the case of other luciferyl compounds calculated. Since a significant dipole moment increase upon excitation is largely responsible for the strong solvent and temperature dependence of the Stokes' shift in LH_2, it is likely that a similar factor is involved in determining the emission maximum of a bioluminescent intermediate in vivo.

The T_1 state of LH_2 has been observed by phosphorescence which is mixed in-plane and out-of-plane polarized. The T_1 state assignment is $^3(\pi,\pi^*)$. The configuration analysis of luciferyl compounds suggests that the T_1 state is either delocalized or localized in one of the ring systems, showing no CT character, in contrast to the fluorescent state.

Acknowledgment. This work was supported by the Robert A. Welch Foundation (D-182) and National Science Foundation (BMS 75-05001). We wish to thank Dr. I. Yamazaki for the original version of the computer programs and for his assistance with the computation.

Appendix

Schematic outline of the CA procedure is given in Figure 9. Arrows represent appropriate matrix transformations. C and $(C^0)^+$ are $n \times n$ unitary matrix and the Hermitian conjugate of the matrix C^0, respectively. B is also a unitary matrix. L is an $i \times j$ matrix involving i and j number of electron configurations (configurations collected in a row vector for the reference and the molecule in question, respectively). U^0 and U are $i \times i$ and $j \times j$ unitary matrix, respectively. The superscript 0 signifies the reference molecule(s), while "no superscript" refers to the molecule(s) for CA. For details, see ref 13.

References and Notes

(1) (a) W. D. McElroy, M. DeLuca, and J. Travis, *Science*, **157**, 150 (1967); (b) W. D. McElroy, H. H. Seliger, and E. H. White, *Photochem. Photobiol.*, **10**, 153 (1969); (c) W. D. McElroy and M. DeLuca in "Chemiluminescence and Bioluminescence", M. J. Cormier, D. M. Hercules, and J. Lee, Ed., Plenum Press, New York, N.Y., 1973, pp 285–311.
(2) (a) T. A. Hopkins, H. H. Seliger, E. H. White, and M. W. Cass, *J. Am. Chem. Soc.*, **89**, 7148 (1967); (b) E. H. White, E. Rapoport, T. A. Hopkins, and H. H. Seliger, *ibid.*, **91**, 2178 (1969); (c) E. H. White, E. Rapoport, H. H. Seliger, and T. A. Hopkins, *Bioorg. Chem.*, **1**, 92 (1971); (d) E. H. White, J. D. Miano, and M. Umbreit, *J. Am. Chem. Soc.*, **97**, 198 (1975); (e) E. H. White and B. R. Mranchini, *ibid.*, **97**, 1243 (1975).
(3) F. McCapra, Y. C. Chang, and V. F. Francois, *Chem. Commun.*, 22 (1968).
(4) (a) N. S. Suzuki and T. Goto, *Tetrahedron Lett.*, 2021 (1971); (b) N. Suzuki, M. Sato, K. Okada, and T. Goto, *Tetrahedron*, **28**, 4065 (1972).
(5) M. DeLuca and M. E. Dempsey, *Biochem. Biophys. Res. Commun.*, **40**, 117 (1970); however, see ref 2d.
(6) R. A. Morton, T. A. Hopkins, and H. H. Seliger, *Biochemistry*, **8**, 1598 (1969).
(7) E. H. White, F. McCapra, and G. F. Field, *J. Am. Chem. Soc.*, **85**, 337 (1963).
(8) W. W. Mantulin and P. S. Song, *J. Am. Chem. Soc.*, **95**, 5122 (1973).
(9) (a) R. Pariser and R. G. Parr, *J. Chem. Phys.*, **21**, 466, 767 (1953); (b) J. A. Pople, *Trans. Faraday Soc.*, **49**, 1375 (1953).
(10) Q. Chae and P. S. Song, *J. Am. Chem. Soc.*, **97**, 4176 (1975).
(11) N. Mataga and K. Nishimoto, *Z. Phys. Chem. (Frankfurt am Main)*, **13**, 140 (1957).
(12) D. Dennis and R. H. Stanford, Jr., *Acta Crystallogr., Sect. B*, **29**, 1053 (1973).
(13) (a) H. Baba, S. Suzuki, and T. Takemura, *J. Chem. Phys.*, **50**, 2078 (1969); (b) H. Baba and I. Yamazaki, *J. Mol. Spectrosc.*, **44**, 118 (1972); (c) S. Suzuki, T. Fujii, and H. Baba, *ibid.*, **47**, 243 (1973).
(14) V. L. Levshin, *Z. Phys.*, **32**, 307 (1925).
(15) F. Perrin, *Ann. Phys.*, **12**, 169 (1929).
(16) H. H. Seliger and R. A. Morton, *Photophysiology*, **4**, 253 (1968).
(17) A. Weller, *Prog. React. Kinet.*, 1, 187 (1961).
(18) L. J. Bowie, R. Irwin, M. Loken, M. DeLuca, and L. Brand, *Biochemistry*, **12**, 1852 (1973).
(19) N. G. Bakhshiev, *Opt. Spektrosk.*, **16**, 821 (1964).
(20) A. Chamma and P. Viallet, *C. R. Acad. Sci. Paris, Ser. C*, **270**, 1901 (1970).
(21) M. Sun, Ph.D. Dissertation, Texas Tech University, 1974.
(22) An Onsager radius of 7.9 Å (~length of the molecular long axis of π-electron system) and parallel orientations of both μ_0 and μ_{S_1} are assumed. The latter assumption is theoretically valid, as the angle between the two dipoles is predicted to be only 10° (Figure 2).
(23) B. Bitler and W. D. McElroy, *Arch. Biochem. Biophys.*, **72**, 358 (1957).